eprints@whiterose.ac.uk
https://eprints.whiterose.ac.uk/

Accepted Manuscript

The relationship between particle morphology and rheological properties in injectable nano-hydroxyapatite bone graft substitutes

Y. Ryabenkova, A. Pinnock, P.A. Quadros, R.L. Goodchild, G. Möbus, A. Crawford, P.V. Hatton, C.A. Miller
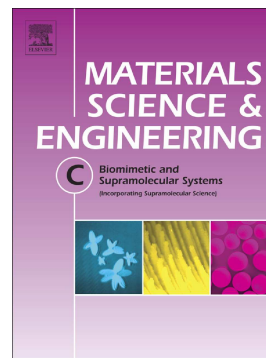
Please cite this article as: Y. Ryabenkova, A. Pinnock, P.A. Quadros, R.L. Goodchild, G. Möbus, A. Crawford, P.V. Hatton, C.A. Miller , The relationship between particle morphology and rheological properties in injectable nano-hydroxyapatite bone graft substitutes. The address for the corresponding author was captured as affiliation for all authors. Please check if appropriate. Msc(2017), doi: 10.1016/j.msec.2017.02.170

The relationship between particle morphology and rheological properties in injectable nano-hydroxyapatite bone graft substitutes.

Y. Ryabenkova[a*], A. Pinnock[b], P.A. Quadros[c], R.L. Goodchild[d], G. Möbus[a], A. Crawford[b], P.V. Hatton[b], C.A. Miller[b]

[a]Department of Materials Science and Engineering, University of Sheffield, UK

[b]School of Clinical Dentistry, University of Sheffield, UK

[c]Fluidinova S.A., Moreira da Maia, Portugal

[d]Ceramisys Ltd., Sheffield, UK

*corresponding author. Email: y.ryabenkova@bradford.ac.uk

Email addresses:

Y. Ryabenkova: Y.Ryabenkova@bradford.ac.uk

A. Pinnock: a.pinnock@sheffield.ac.uk

P.A. Quadros: paulo.quadros@fluidinova.com

R.L. Goodchild: r.goodchild@ceramisys.com

G. Möbus: g.moebus@sheffield.ac.uk

A. Crawford: a.crawford@sheffield.ac.uk

P.V. Hatton: paul.hatton@sheffield.ac.uk

C.A. Miller: c.a.miller@sheffield.ac.uk

*corresponding author: Yulia Ryabenkova y.ryabenkova@bradford.ac.uk (or y.ryabenkova@sheffield.ac.uk), Department of Materials Science and Engineering, University of Sheffield, Sir Robert Hadfield Building, Mappin Street, Sheffield, S1 3JD, UK,

Phone: +44 (0) 1142 225959

Abstract

Biomaterials composed of hydroxyapatite (HA) are currently used for the treatment of bone defects resulting from trauma or surgery. However, hydroxyapatite supplied in the form of a paste is considered a very convenient medical device compared to the materials where HA powder and liquid need to be mixed immediately prior to the bone treatment during surgery. In this study we have tested a series of hydroxyapatite (HA) pastes with varying microstructure and different rheological behaviour to evaluate their injectability and biocompatibility. The particle morphology and chemical composition were evaluated using HRTEM, XRD and FTIR. Two paste-types were compared, with the HA particles of both types being rod shaped with a range of sizes between 20-80 nm while differing in the particle aspect ratio and the degree of roundness or sharpness. The pastes were composed of pure HA phase with low crystallinity. The rheological properties were evaluated and it was determined that the pastes behaved as shear-thinning, non-Newtonian liquids. The difference in viscosity and yield stress between the two pastes was investigated. Surprisingly, mixing of these pastes at different ratios did not alter viscosity in a linear manner, providing an opportunity to produce a specific viscosity by mixing the two materials with different characteristics. Biocompatibility studies suggested that there was no difference in *in vitro* cell response to either paste for primary osteoblasts, bone marrow mesenchymal stromal cells, osteoblast-like cells, and fibroblast-like cells. This class of nanostructured biomaterial has significant potential for use as an injectable bone graft substitute where the properties may be tailored for different clinical indications.

Highlights

- Rheological studies of non-setting water-based nano-hydroxyapatite pastes with varying morphology have shown that they are non-Newtonian shear-thinning fluids.

- No dispersant has been used to control handling properties.

- When mixing various ratios of the two materials with different morphology the viscosity of the resulting pastes does not follow the rule of mixtures.

- Biocompatibility studies showed excellent *in vitro* cell response for all the pastes on a variety of cell types tested.

1 Introduction

Hydroxyapatite (HA) is an important calcium phosphate bioceramic with the chemical formula $Ca_{10}(PO_4)_6(OH)_2$. Poorly crystalline rod-like nano-hydroxyapatite is the main mineral component of bone where it is dispersed in the matrix of collagen fibrils, and it amounts up to 65% of total bone mass of the vertebrates [1, 2]. Synthetic hydroxyapatite mimics some of the features of a biological apatite and has significant potential to be an excellent bone replacement material due to its exceptional biocompatibility and osteoconductivity [3, 4]. Hydroxyapatite-containing biomaterials are therefore widely employed for the treatment of bone defects [5, 6]. Most commercial systems are presented as macro-scale particles or blocks, and it is only relatively recently that nanoscale hydroxyapatite and related materials have found wider clinical use in an injectable form. In the early 1980s, one approach to obtain an injectable material was to use one or more calcium orthophosphate compounds and water (or aqueous solution) as starting materials, and to introduce these precursors into the bone defect area via a delivery device (normally a syringe) where they eventually underwent transformation into a monolithic hydroxyapatite via self-setting in the cavity [7-9]. Subsequently, an alternative approach was to combine a hydroxyapatite powder with an additive (normally organic dispersants to prevent agglomeration of the ceramics) to improve its injectability properties [10]. In this case, no setting reaction occurred but a relatively high pH was required to stabilise the suspension [11].

While these earlier forms of hydroxyapatite have made a significant contribution to bone surgery for many decades, they have each suffered from limitations or drawbacks. Block and larger particulate devices are not injectable making them more difficult to place, and in some sites there is a greater risks of exfoliation or infection. Calcium phosphate cements offer opportunities for minimally invasive procedures and injection, but some formulations have suffered from serious biocompatibility issues including embolism and injuries to patients during surgery [12].

4

More recently, a number of commercial injectable materials based on the combination of nanoscale hydroxyapatite and water have been launched onto the market that do not suffer from the serious drawbacks associated with calcium phosphate and related cements. Published data is encouraging, with evidence of good biocompatibility, osteoconductivity, and excellent safety [13, 14]. While a number of papers now describe the preparation of nanohydroxyapatite systems and their properties [14, 15], there have been no detailed studies that combine rheological and morphological investigations to better understand structure-property relationships in this new class of biomimetic medical device.

Thus, we prepared novel water-based non-setting hydroxyapatite pastes similar to those that are commercially available as bone graft substitutes. These pastes do not require the addition of organic solvents or dispersants to stabilise the colloidal system in order to prevent setting, ageing or phase separation during the injection. The main aim of this research was therefore to investigate the morphological and rheological properties of these nanoscale hydroxyapatite pastes, allowing for tailored viscosities which match the requirements of clinicians for various indications in dental and orthopaedic surgery. As a result, we attempted to identify approaches to better control injectability by changing particle size and shape of the constituent hydroxyapatite without detriment to biocompatibility.

2 Materials and methods

2.1 Nano-hydroxyapatite preparation

Materials for this study were prepared as described in [16]. Aqueous solutions of calcium chloride dihydrate $CaCl_2 \cdot 2H_2O$ (Sigma), chosen as a source of Ca^{2+} ions, and potassium phosphate monobasic KH_2PO_4 (assay > 99.0%, Sigma) as a source of PO_4^{3-} ions were fed into the inlets of the NETmix®

reactor [17] at the Ca/P molar ratio of 5:3 under controlled pH conditions (pH = 11-12 which was adjusted using KOH aqueous solution (assay > 85.0% pellets, Sigma)). The concentration of KOH used for the pH adjustment was the same for all the materials prepared. The resulting slurries were washed several times in order to remove the residual K^+ and Cl^- ions and further concentrated to reach a condition of a viscous paste with the final concentration of 38 wt% for all materials studied. The pastes were given codes BP-1 (synthesised at 30±1°C) and BP-2 (synthesised at 27±1°C), differing from one another at nano-level in particles size and shape, as well as in rheological properties. The equality of the solid content loading (in wt%) for both BP-1 and BP-2 pastes was verified using thermogravimetric analysis (vide infra).

A proportion of both materials were dried at 60 °C and ground in agate mortar and pestle for morphological studies. An aliquot of the materials was calcined in a furnace at 1000 °C for 2 hours (at heating rate of 10 °C·min^{-1}) in order to evaluate their thermal stability.

2.2 Materials characterisation

Fourier Transform Infrared (FTIR) spectra were acquired using Bruker ALPHA's Platinum Attenuated Total Reflectance (ATR) FTIR spectrometer equipped with a single reflection diamond ATR module. The spectra were recorded in the absorbance mode from 4000 to 375 cm^{-1} at 1 cm^{-1} resolution averaging 128 scans.

X-ray powder diffraction (XRPD) patterns were acquired using a Siemens D5000 Diffractometer operating at 40 kV and 40 mA with Cu K_α radiation. Both paste materials and calcined powders were examined using an X-ray transparent Poly(methyl methacrylate) (PMMA) sealed cap sample holder. Analysis of the obtained patterns was carried out using X'Pert HighScore Plus software, and stripping of the $K_{\alpha-2}$ component was carried out when appropriate.

Samples for the transmission electron microscopy (TEM) characterisation were prepared by dispersing a dry powder of BP-1 and BP-2 onto a holey carbon film supported by a 300 mesh copper

TEM grid. A JEOL JEM-3010 TEM with a LaB_6 electron gun was used to obtain images of the agglomerated hydroxyapatite particles at an accelerating voltage of 300 kV. High resolution images of the individual nanoparticles were obtained using field emission gun JEOL JEM 2010F TEM at an accelerating voltage of 200 kV. Particle size analysis including evaluations of the aspect ratios and/or projected areas has been performed using ImageJ software for at least 200 particles for each material.

Thermogravimetric analysis (TGA) was carried out using a PerkinElmer Pyris 1 thermogravimetric analyser. Heating was performed in a platinum crucible in air flow (20 $cm^3 \cdot min^{-1}$) at a rate of 10 °C min^{-1} up to 1000 °C.

The rheological properties, including viscosity and yield stress, of the pastes were tested using an Anton Paar MCR 301 modular compact rheometer in rotational mode. Rheological tests were conducted at different temperatures (0, 10, 20, 37 °C) with at least three replicates performed for each test. Approximately 1 cm^3 of material was used to perform the experiments in a plate-plate geometry assembly of the instrument (diameter = 25 mm) with the gap between parallel plates set at 1.3 mm.

2.3 Cell culture and PrestoBlue® assay

Reagents were purchased from Sigma-Aldrich unless otherwise stated. Human osteoblast-like cells, the osteosarcoma cell line (MG-63), mouse myoblast cell line (C2C12) and mouse fibroblast-like (L929) cells were cultured in Dulbecco's Modified Eagles Medium (DMEM). 1 % (v/v) non-essential amino acids was added to culture media for MG-63 cells. Human osteogenic sarcoma cell line, Saos-2 (osteoblast-like) cells were cultured in McCoy's 5a medium. Rat osteosarcoma (ROS) cells were cultured in minimal essential medium (alpha modification). Human osteoblast (HOBs) cells were cultured in osteoblast growth medium (PromoCell) and human bone marrow-derived mesenchymal stem cells (hBM-MSCs) were cultured in NH expansion medium (Miltenyi Biotec). All culture media contained 50 $U.ml^{-1}$ penicillin and 50 $\mu g.ml^{-1}$ streptomycin. With the exception of BM-MSC and HOB

7

culture media, foetal calf serum (FCS) was added to culture media to a final concentration of 10%. All the cell types were cultured at 37 °C and 5 % CO_2/95 % air and were passaged at 80-90 % confluence. For experimental use, the cells were seeded into 24 well plates. To assay for cytocompatibility, 1 cm lengths of gamma sterilised BP-1 and BP-2 pastes (8.53 ± 1.19 mg paste average wet weight, volume = 236 mm^3) were incubated overnight in culture medium containing 10% FCS (1 cm paste/1 ml medium). The conditioned media was added to pre-seeded monolayers of $1x10^5$ cells and the cultures incubated for 24 or 48 hours at 37 °C (as indicated in the ISO 10993-5:2009 recommendations). Cell viability was determined using PrestoBlue® (Invitrogen) according to the manufacturer's instructions. In this assay, living metabolically active cells convert the resozurin dye to the reduced form of resorufin which is fluorescent and can be determined spectrophotometrically. In brief, the PrestoBlue® was diluted 1:9 in culture medium, added to the cell cultures which were incubated at 37 °C. 200 µl samples of the culture media were removed after 1-2 hours (depending on the cell type) and the relative fluorescence was determined (Infinite 200, Tecan, Reading, UK) at wavelengths of 560 nm and 590 nm for excitation and emission respectively.

3 Results

3.1 Materials characterisation

The most common and informative techniques for a comprehensive evaluation of the chemical composition and structure of the materials used in the bioceramic research area are: X-ray methods (XRD), spectroscopic tools (FTIR or Raman), microscopy (TEM or SEM), thermal methods (TGA) as well as rheometer for evaluation of viscosity and flowability properties [18, 19].

3.1.1 Attenuated total reflectance – Fourier transform infrared spectroscopy (ATR-FTIR)

Fig. 1 shows the ATR-FTIR spectra of both BP-1 and BP-2 materials. Most of the active bands which are located in the area between 1200 and 400 cm^{-1} match previously reported data for hydroxyapatite, and are compatible with the imperfect microstructure found by the other techniques. Thus, the region between 1200-900 cm^{-1} is typical for phosphate stretching, 600 cm^{-1} for phosphate bending, whereas 3571 and 632 cm^{-1} are that of hydroxyl vibrations [20-22]. The broad band in the region between 3500 and 3000 cm^{-1} is assigned to water vibrations. Interestingly, carbonate substitution was also detected in both samples. This corresponds to the peaks of 870 cm^{-1} and to the region of 1600 to 1300 cm^{-1} that is typical for the bending and stretching modes of the CO_3^{2-} group respectively.

3.1.2 X-Ray powder diffraction (XRPD)

The XRPD patterns of the BP-1 and BP-2 pastes as well as calcined powders are given in Fig. 2. The results indicated that the only phase present in the paste samples (Fig. 2 a, b) was partially crystalline hydroxyapatite (HA) with a full match to JCPDS entry 9-432 represented by broad peaks. Pure hydroxyapatite was also detected in the calcined materials (Fig. 2 c, d). The sharpening of peaks and reduction of background level during calcination is indicative of the changes in materials crystallinity, which includes both grain growth and crystallisation of amorphous domains.

3.1.3 Thermogravimetric analysis (TGA)

The results of the thermogravimetric analysis are shown in Fig. 3. A rapid weight loss was observed between room temperature and 400 °C for both BP-1 and BP-2 pastes (BP-2 results were identical to BP-1 and only the former is shown) which is characteristic of the release of water from the surface and lattices of hydroxyapatite particles. Above this temperature after the loss of all the liquid both BP-1 and BP-2 materials maintained constant weight of 38 wt% of dry component with no obvious signs of decomposition detected, except for a very small weight loss above 800 °C characteristic for the decomposition of carbonates. The two materials were identical to each other in terms of thermal behaviour and were thermally stable over the wide range of temperatures.

3.1.4 Transmission electron microscopy (TEM)

Fig. 4a and 4b show micrographs of the BP-1 and BP-2 materials, and high resolution images are given in Fig. 4c and 4d. As can be seen from the TEM analyses of both BP-1 and BP-2 materials, a range of particle size and shapes were observed. Rod shaped particles of approximately 20-80 nm are seen dominating for both materials; BP-2 particles are notably finer with smaller rod diameter and more sharply pointed ends, as well as smaller particle volume on average. HRTEM images of the nano-hydroxyapatite particles reveal partially crystalline structure with inclusions of amorphous domains in both materials. Examples of amorphous (Fig. 4c) and crystalline regions (Fig. 4d) are encircled.

Fig. 5a shows the projected areas histograms for both BP-1 and BP-2 materials (calculations based on the approximation that particles are symmetrical ellipses). It is apparent that the mean area for BP-1 is noticeably higher than for BP-2 suggesting that the former particles are intrinsically bigger in size. Fig. 5b, in turn, shows the aspect ratio evaluations where the longest and the shortest axes of BP-1 and BP-2 materials were plotted against each other. The black diagonal corresponds to a circle. Both pastes have a great variety of aspect ratios from 1:1 to 10:1. BP-1 is characteristic by a large number of particles between the 1:1 and 2:1 ratio, while the paste BP-2 has accumulations of particles on the one hand between spherical and 2:1 ratio, but also having some exceptionally high aspect ratios above 4:1.

3.1.5 Rheological studies

The results of one the most typical rheological tests, where the material is subjected to a constant shear of 10 s^{-1} and the measurements are taken at certain intervals, are reported in Fig. 6. The changes of viscosity with time as well as the presence of the yield stress are characteristic of non-Newtonian shear-thinning materials. Interestingly, the initial viscosity and therefore the yield stress of the material made of smaller and more rounded nano-particles (BP-2) were 10 times higher than

10

that of the larger particles (BP-1) thus indicating the effect of the size and geometry of the constituent particles on the rheological properties of the material.

Further experiments were conducted on the BP-1 paste as it possessed lower initial viscosity compared to BP-2 and therefore was easier to handle. The rheological behaviour was investigated at variable shear rates (0 to 1000 s^{-1}) and the measurements were performed at different temperatures. The influence of the heating/cooling of the paste on its viscosity/yield stress is shown in Table 1.

Surprisingly, the resistance to flow of the BP-1 paste increased with the increase in temperature. More generally, the fluidity of the material improved after cooling the paste. There is some degree of uncertainty about the linearity of this dependence, however, the general trend of the observed increase of the yield stress with increasing the temperature was distinct and reproducible.

Increase of stiffness upon heating was also found for BP-2, however, no quantitative value was available at the upper temperature due to excessive stiffness. The trend of viscosity decrease with lowering temperature is therefore general for both kinds of these non-setting water based nanoceramics systems.

As different fluidity of the materials may be preferred when performing different types of surgery, the possibility to control the initial viscosity and, in turn, the handling properties of the pastes were further explored. BP-1 and BP-2 pastes were mixed with each other at different ratios (at the stage of the slurries to provide a homogeneous mixing) and the initial viscosity was measured (see Fig. 7).

Another interesting and unexpected observation can be seen from these results. A non-linear change in the initial viscosity with mixing ratio has been detected which we call the "majority-paste effect". In other words, the presence of the paste in the highest concentration has an over-proportionate influence on the resulting viscosity of the mixture. No significant phase separation

(evaluated by visual inspection of the pastes) was observed during the rheological tests and the evaporation of the solvent is excluded.

3.2 Biological evaluation

The cytocompatibility of the nanopastes was determined using an assay protocol based on the standard *ISO 10993-5:2009* recommendations. The nanopaste was soaked in media for 24 hours and then the conditioned media removed and incubated with the following cell types for 24 or 48 hours: hBM-MSCs and primary HOBs, osteoblast-like cells (MG63, Saos-2 and ROS cell lines) and L929 and C2C12 cell lines. The nano-paste conditioned media were found to have no significant effect on the metabolic activity of hBM-MSCs, MG63, Saos-2 or C2C12 cells after 24 h of incubation with the cells (Fig. 8a). A relatively small but significant inhibitory effect of up to 30% was observed on the metabolic activity of HOB, ROS and L929 cells ($p > 0.05$, Fig 8b). Incubating the cell types for a longer period with the paste-conditioned media gave very similar results (therefore not shown on Fig. 8). For example, compared to the control cultures, hBM-MSCs had 97.8 ± 6.4% activity, HOBs showed 86.4 ± 4.4%, L929 cells had 68.4 ± 5.9% and ROS cells showed 70.8 ± 17.3% activity after 48 h incubation with the paste-conditioned media. BP-1 and BP-2 showed similar effects on the metabolic activity of the various cell types. A comparison of BP-1 and BP-2 on MG63 cells is shown in Fig. 8b.

4 Discussion

Injectable non-setting nanoscale water based hydroxyapatite pastes were examined by an array of characterisation techniques aimed at the determination of composition, structure-activity correlations as well as the biological response when introducing these materials into the mammalian cell culture. The viscosity and in turn injectability properties of these materials were of a particular interest, therefore it was decided to evaluate how the properties of the materials at nano-scale influence their macroscopic, and in particular rheological, behaviour.

12

4.1 Morphological studies

The hard tissue in vertebrates is predominantly made of the nanocrystalline hydroxyapatite inorganic phase (>65%) with small inclusions of carbonate anions [1], and it is this mineral content that is responsible for the bone's rigidity and toughness. In order to mimic the bone tissue, a bone graft substitute should be made of a nano-dimensional inorganic calcium phosphate phase that also has small amounts of incorporated carbonate groups.

A range of techniques were employed to examine the chemical composition and structural differences of the pastes. XRD analysis showed that both BP-1 and BP-2 pastes were made of a pure nano-hydroxyapatite phase (with significant peak broadening and raised background indicative of small crystallite size and the presence of an amorphous phase respectively), and ATR-FTIR confirmed the presence of a carbonate group in the material (Fig. 1). Despite carbonate ions not being deliberately added during the preparation process, there are cases that report CO_2 capture from air when the ceramics is being prepared at high values of pH [23]. A second hint supporting the presence of carbonate groups comes from the TGA analysis (Fig. 3) that mimicked the calcination process, when during the heat treatment there was rather small but traceable weight loss (in the range of 800-900 °C). Carbonate (CO_3^{2-}) groups were detected in samples using ATR-FTIR as shown in Fig. 1. It is known that ATR-FTIR is a surface technique with the penetration depth ranging from 0.3-5 microns [24], whereas XRD is normally referred to as a bulk technique. As it was possible to detect the presence of CO_3^{2-} groups in the samples but no other phase was detected by the XRD (Fig. 2), it is likely that carbonate ions are present on the surface of the constituent hydroxyapatite particles in the form of thin solid layers. XRD and TGA results together suggested that the nano-hydroxyapatite pastes were near-stoichiometric thermally stable materials that did not decompose into tricalcium phosphate when heated up to 1000°C. TGA data also revealed that the ceramic loading was *ca.* 38% for both BP-1 and BP-2 pastes. This makes the rheological behaviour of the two materials dependant on only one parameter, namely geometry of the constituent particles

13

(determined by TEM), as chemical composition and water content are in this case identical between BP-1 and BP-2.

To further demonstrate the pastes nano-crystalline nature, TEM was used to investigate differences between BP-1 and BP-2 materials at the nanoscale. The high resolution images (Fig. 4 c-d) obtained by HRTEM show that both materials were made of polycrystalline nanoparticles contained nano-crystallites of *ca.* 5 nm in diameter surrounded by amorphous pockets. The conventional TEM imaging showed that the particle size and shape were slightly different between the two materials (Fig. 4 a-b). The difference in particle size is more noticeable than the difference in aspect ratio on average. It is likely that this difference contributes to the variations in the rheological behaviour of these materials and we discuss it in the section below.

Regarding the difference in particle shape and size for the materials prepared at different temperatures, this is a well-known phenomenon and has been widely described in the literature for inorganic nanoparticles. Notable examples include Cu [25] and CuO [26] nanoparticles prepared by temperature controlled method, where they develop various nanostructure architectures depending on the temperature used during the preparation. Cobalt ferrite ($CoFe_2O_4$) nanoparticles [27] can also be prepared in various shapes and sizes depending on the synthesis temperature. In these cases the trend of the change in particles size is as follows: the higher is the temperature, the bigger are the resulting particulate. The same dependence is preserved in our case, as on average BP-1 particles have a noticeably higher cross sectional area compared to the BP-2 material (Fig. 5a).

This observation may be explained either by the Ostwald ripening and Gibbs-Thomson effect [28, 29] or by oriented attachment [30]. The Ostwald ripening effect is responsible for the last phase of transition between liquid precursors into a solid hydroxyapatite particulate. When affected by a temperature increase, the smaller aggregates that have not reached the critical nucleus size can be easily dissolved due to their thermodynamic instability. This denucleation process of particles with sub-critical nucleus size eventually leads to the formation of larger particles at higher temperature,

and vice versa – particles of smaller sizes at lower temperatures. The oriented attachment, in turn, is a process that corresponds to the evolution of the particle size, mostly coarsening, due to the growth of the neighbouring particles that are crystallographically oriented in the same direction.

It has been reported that more than one mechanism is normally responsible for the crystal growth [30], with the former corresponding to the dissolution of the smaller particles and the latter with the merging of the smaller crystallites. We do not therefore exclude the possibility of both mechanisms taking place when changing the synthesis temperature of hydroxyapatite. Furthermore, there may be other factors that could potentially influence the particle growth rate besides the temperature effects such as the geometry of the microfluidic reactor and reagent flow compared to the static batch methods.

4.2 Rheological behaviour

The rheological properties of the bone graft substitute are a crucial factor for efficient surgical delivery. Injectable synthetic bone graft materials ideally should have the following properties: i) to have such fluidity properties to be able to fill the gaps of the whole bone defect and ii) to be non-phase separating during the extrusion from the delivery device and to be relatively easy to handle. It should be noted that in our study we do not define injectability as ratio of the mass expelled from the syringe to the total mass before injecting [31]. Instead, we refer to it as "capacity to stay homogeneous during injection, independently of the injection force." [32] By using the latter definition and in order to understand how to control the rheological behaviour of the hydroxyapatite water based pastes we have performed a series of tests using a rheometer in the rotational mode at different temperatures and different shear rates. The tests at a constant shear (Fig. 6) showed that the material BP-1 had lower initial viscosity compared to the smaller particles of BP-2 paste. This can be explained by inter-particulate interactions between the layers of the nano-HA in the aqueous solution [15]. Thus, the specific surface area of the smaller particles (BP-2) will be higher than that of

the larger particles (BP-1). The contact area open for electrostatic/van der Waals interactions between the particles is therefore also higher, which in turn results in the higher viscosity of the BP-2 material. Shape and size of the particles both contribute, as higher elongation at same volume, should lead to more interaction due to higher surface area.

In our case, particles constituting BP-1 and BP-2 have been approximated to be perfect ellipsoids with the longest and the shortest axes (D2 and D1 respectively, Fig. 5b). As we experimentally observed BP-2 being more viscous than BP-1, we therefore conclude that the effect of particle size is dominant and can be an explanation for our viscosity differences between the two materials. Further contributions to the strength of particle agglomeration would come from surface-roughness, non-convexity of particle shapes, and hierarchy of cluster-agglomeration, not accounted for in the elliptical modelling.

Steady rheological tests at variable shear rates and temperatures performed for the BP-1 paste revealed a drop in the viscosity upon cooling (Table 1). The observation of the decrease in the viscosity with decrease in temperature is somewhat counterintuitive (provided that the solvent evaporation effect is excluded for our systems), however, some research groups have reported similar phenomenon. Silberberg *et al.* [33] reported to have observed the decrease of the intrinsic viscosity with the drop in temperature when studying diluted and concentrated aqueous solutions of some acrylate polymers. They hypothesised that the reason behind this effect may due to either changes in solvent power coupled with the exceptional gelling tendency of polymer, or due the formation of hydrogen bonds. Nguyen *et al.*, in turn, have observed drastic changes in rheological behaviour beyond critical temperature range of 55-70 °C for the inorganic nano-particles suspensions in water (known as nanofluids) [34, 35]. They attribute this phenomenon to the deterioration of the particles suspension properties occurring during changes in temperature.

It is assumed that both explanations are applicable to our systems, as they consist of high concentrations of inorganic nano-particles suspended in water. However, HA and water both

possess chemical groups that can be both hydrogen bond donors and acceptors. Moreover, the HA particles are assumed to be surrounded by a few layers of water [36], and therefore the impact of the hydrogen bonding between the solvent and solute must also be taken into consideration when describing the rheological behaviour of such systems.

The surface charge, or zeta-potential, of the material can also be a factor that can help to assess the rheological behaviour [37]. For viscous hydroxyapatite suspensions in water it normally has a negative value [38] unless the pH of the material is modified or certain deflocculants are added [39] to prevent agglomeration and to stabilise the particles in the liquid phase. As we do not introduce any additional component into our bi-phasic system, it seems that in our case it is possible that the particle shape and size may have an effect on the surface charge and therefore influence the viscosity measurements. Most likely, in our materials the inter-particle repulsion forces, as well as the layers of water surrounding each particle, prevent agglomeration and also allow the pastes to flow. However, the fluidity is different between the two materials due to the differences in particle geometry which determines the amount of functional groups exposed on the surface. The presence of functional groups and water layers leads to a formation of an energy barrier created by the equilibrated van der Waals attractive and electrical double layer repulsive forces between the particles that stabilises the system and prevents coagulation.

As we aimed to assess the possibility of controlling the viscosity, and therefore injectability, of the material, it was decided to combine the BP-1 and BP-2 materials to evaluate the resulting viscosity of the mixes. As described in section 3.1.5 it is a homogeneous mixture due to mixing occurring at the stages of diluted slurry and therefore the formation of discrete domains can be excluded. Interestingly, after the addition of a material with higher viscosity to the material with lower viscosity at ratio 1:3 (Fig. 7) the resulting viscosity value did not follow the rule of mixtures and therefore did not lie in centrally between the values of the paste containing just one type of the material and the paste containing two materials at a ratio of 1:1. On the contrary, it appeared to be

closer to the value of the "majority-paste" thus suggesting that the changes in the electrostatic interactions between the particles are non-linear with the addition of the particles with higher surface area. The addition of the paste with lower viscosity to a paste with higher viscosity in the ratio of 1:3 does not significantly differ from a 1:1 ratio of the pastes, suggesting the lower impact of the less viscous BP-1 paste when introducing it to the higher viscosity BP-2 paste.

These results suggest that in order to reach the desired handling properties of the shear thinning pastes during surgery, a simple mixing of the initial materials with known viscosities will not result in a linear change of this parameter. We believe that the "majority paste" phenomenon is much more complicated and would require significant further studies on electrostatic interactions of the particles in order to fully control the injectability of the materials.

4.3 Cell culture

The nano-paste conditioned media had caused a small but significant inhibition of metabolic activity in HOB, ROS and L929 cells. No significant effects were observed on the other cell types used. It is widely reported in the literature that, under certain culture conditions and concentration of nano-HA, a small decrease in cellular metabolic activity/increase in cytotoxicity is observed. This is thought to be due to numerous factors including the shape and size of the particles [40-42]. In this study, some inhibition (up to 30%) of metabolic activity (indicative of the viability of the cells) was observed in some cell-types. The reason for this is as yet unknown but might be due to intrinsic differences in membrane morphology, expression of inflammatory cytokines and/or extent of particle-cell association [42, 43] or the stage of cell differentiation.

 As previously discussed, differences in particle morphology and subsequent rheology were observed for BP-1 and BP-2. However, no difference in the cellular response to PrestoBlue® was found suggesting that particle morphology may not play a role in osteoblast cytotoxicity.

5. Conclusions

This paper presents a detailed study of the rheological and morphological properties of non-setting hydroxyapatite pastes that could be considered for use as water-based, nanoceramic medical device for bone tissue regeneration. The pastes were stable, or non-phase-separating, colloid systems that were fabricated solely from nano-HA and water as a solvent, with no dispersants added to improve the injectability. The morphology of the materials was investigated using XRPD, TGA, TEM and ATR-FTIR, indicating that the solid component of the pastes consisted of a stoichiometric nanoscale hydroxyapatite with small inclusions of carbonate. Differences in particles sizes, shapes, and aspect ratios were shown to be determinants of rheological behaviour in the pastes, but at the same time these factors had no significant effect on *in vitro* biocompatibility. This investigation of the rheological behaviour of the pastes showed that the viscosity, and therefore the injectability, can be manipulated by combining the materials with different particle sizes and shapes in order to reach the desired fluidity without the need for additives. It was concluded that this type of nanostructured biomaterial has the potential to be used as an injectable bone graft substitute where the properties may be tailored precisely for different clinical indications.

Acknowledgements

6. References

[1] Vallet-Regi M, Gonzalez-Calbet J. Calcium phosphates as substitution of bone tissues. Prog. Solid State Chem. 2004;32:1-31.

[2] Howard Carter D, Hatton PV, Aaron JE. The ultrastructure of slam-frozen bone mineral. Histochem J, 1997;29:783-793.

[3] Ogilvie A, Frank RM, Benqué EP, Gineste M, Heughebaert M, Hemmerle J. The biocompatibility of hydroxyapatite implanted in the human periodontium. J Periodontal Res. 1987;22:270-283.

[4] Damien E, Hing K, Saeed S, Revell PA. A preliminary study on the enhancement of the osteointegration of a novel synthetic hydroxyapatite scaffold in vivo. J Biomed Materials Res A, 2003;66A:241-246.

[5] Paderni S, Terzi S, Amendola L. Major bone defect treatment with an osteoconductive bone substitute. Musculoskel Surg. 2009;63:89-96.

[6] Uchida A, Araki N, Shinto Y, Yoshikawa Y, Kurisaki E, Ono K. The use of calcium hydroxyapatite ceramic in bone tumour surgery. J Bone Joint Surg Br. 1990;72:298-302.

[7] Xu HH, Weir MD, Burguera EF, Fraser AM. Injectable and macroporous calcium phosphate cement scaffold. Biomater. 2006;27:4279-4287.

[8] Chow LC, Calcium phosphate cements: chemistry, properties and applications. Mat Res Symp Proc. 2000;599:27-37.

[9] Ginebra MP, Fernandez E, De Maeyer EAE, Verbeek RMH, Boltong MG, Ginebra J, Driessens FCM, Planell JA. Setting reaction and hardening of an apatitic calcium phosphate cement. J Dent Res. 1997;76:905-912.

[10] Gardini D, Galassi C, Lapasin R. Rheology of hydroxyapatite dispersions. J Am Cer Soc. 2005;88:271-276.

[11] Bao Y, Senos AMR, Almeida M. Rheological behaviour of aqueous suspensions of hydroxyapatite. J Mater Sci-Mater Med. 2002;13:639-643.

[12] Krebs J, Aebi N, Goss BG, Sugiyama S, Bardyn T, Boecken I, Leamy PJ, Ferguson SJ. Cardiovascular changes after pulmonary embolism from injecting calcium phosphate cement. J Biomed Mater Res B Appl Biomater. 2007; 82:526-532.

[13] Busenlechner D, Huber CD, Vasak C, Dobsak A, Gruber R, Watzek G. Sinus augmentation analysis revised: the gradient of graft consolidation, Clin Oral Implants Res. 2009;44;1078-83.

[14] Huber FX, Berger I, McArthur N, Huber C, Kock HP, Hillmeier J, Meeder PJ, Evaluation of a novel nanocrystalline hydroxyapatite paste and a solid hydroxyapatite ceramic for the treatment of critical size bone defects (CSD) in rabbits. J Mater Sci-Mater Med. 2008;19:33-38.

[15] Bouyer E, Gitzgofer F, Boulos MI, Morphological study of hydroxyapatite nanocrystal suspension. J Mater Sci-Mater Med. 2000;11:523-531.

[16] Brito Lopez JC, Gomez de Queiroz Dias MM, Tenedorio Matos Da Silva VM, Quadros De Oliveira E Santos, PA, Mendes Monteiro FJ, Da Cunha Gomes PJ, Pataquiva Mateus AY International Patent WO2008/007992 A2 (2008)

[17] Brito Lopez JC, Miranda Dos Santos Da Costa PE, Gomez de Queiroz Dias MM, Areosa Martins AA, European Patent EP 1 720 643 B1 (2008)

[18] Tan R, Niu X, Gan S, Feng Q, Preparation and characterization of an injectable composite" J Mater Sci: Mater Med. 2009; 20:1245–1253.

[19] Murugan R, Ramakrishna S. Bioresorbable composite bone paste using polysaccharide based nano hydroxyapatite. Biomater. 2004;25:3829–3835.

[20] Huang LY, Xu KW, Lu J. A study of the process and kinetics of electrochemical deposition and the hydrothermal synthesis of hydroxyapatite coatings. J Mater Sci-Mater Med. 2000;11:667-673.

[21] Lim GK, Wang J, Ng SC, Gan LM. Nanosized hydroxyapatite powders from microemulsions and emulsions stabilized by a biodegradable surfactant. J Mater Chem. 1999;9:1635-1639.

[22] Gibson IR, Rehman I, Best SM, Bonfield W. Characterization of the transformation from calcium-deficient apatite to beta-tricalcium phosphate. J Mater Sci-Mater Med. 2000;11;799-804.

[23] Viswanath B, Ravishankar N. Controlled synthesis of plate-shaped hydroxyapatite and implications for the morphology of the apatite phase in bone. Biomater. 2008;29:4855-4863.

[24] Jabbari E, Wisniewski N, Peppas NA. Evidence of mucoadhesion by chain interpenetration at a poly(acrylic acid)/mucin interface using ATR-FTIR spectroscopy. J. Control. Release 1993;26:99-108.

[25] Mott D, Galkowski J, Wang L, Luo j, Zhong C-J. Synthesis of Size-Controlled and Shaped Copper Nanoparticles. Langmuir, 2007;23;5740-5745.

[26] Liu X, Geng B, Du Q, Ma J, Liu X. Temperature-controlled self-assembled synthesis of CuO, Cu2O and Cu nanoparticles through a single-precursor route. J Mater Sci Eng A 2007;448:7-14.

[27] Kima YI, Kim D, Lee CS. Synthesis and characterization of CoFe2O4 magnetic nanoparticles prepared by temperature-controlled coprecipitation method. Physica B Condens Matter 2003;337:42-51.

[28] Madras G, McCoy BJ. Temperature effects during Ostwald ripening. J. Chem. Phys. 2003;119:1683-1693.

[29] Madras G, McCoy BJ. Temperature effects on the transition from nucleation and growth to Ostwald ripening. Chem Eng Sci. 2004;59:2753-2765.

[30] Xue X, Lee Penn R, Leite ER, Huang F, Lin Z. Crystal growth by oriented attachment: kinetic models and control factors. CrystEngComm. 2014;16:1419-1429.

[31] Qi X, Ye J. Mechanical and rheological properties and injectability of calcium phosphate cement containing poly (lactic-co-glycolic acid) microspheres. Mater Sci Eng C 2009;29:1901–1906.

[32] Bohner M, Baroud G. Injectability of calcium phosphate pastes, Biomater. 2005;26:1553–1563.

[33] Silberberg A, Eliassaf J, Katchalsky A. Temperature dependence of light scattering and intrinsic viscosity of hydrogen bonding polymers. J Polym Sci. 1957;23:259-284.

[34] Nguyen CT, Desgranges F, Roy G, Galanis N, Maré T, Boucher S, Angue Mintsa H. Temperature and particle-size dependent viscosity data for water-based nanofluids – hysteresis phenomenon. Int J Heat Fluid Fl. 2007;28:1492-1506.

[35] Nguyen CT, Desgranges F, Galanis N, Roy G, Maré T, Boucher T, Angue Mintsa H. Viscosity data for Al2O3-water nanofluids – hysteresis: is heat transfer enhancement using nanofluids reliable? Int J Therm Sci. 2008;47:103-111.

[36] Corno M, Rimola A, Bolis V, Ugliengo P. Hydroxyapatite as a key biomaterial: quantum-mechanical simulation of its surfaces in interaction with biomolecules. Phys Chem Chem Phys. 2010:12:6309-6329.

[37] Knowles JC, Callcut S, Georgiou G. Characterisation of the rheological properties and zeta potential of a range of hydroxyapatite powders. Biomater 2000;21:1387-1392.

[38] Zhang Y, Zhou K, Bao Y, Zhang D. Effects of rheological properties on ice-templated porous hydroxyapatite ceramics. Mater Sci Eng C. 2013;33:340-346

[39] Bouyer E, Gitzhofer F, Boulos MI. Morphological study of hydroxyapatite nanocrystal suspension. J Mater Sci-Mater Med. 2000;11;523-531.

[40] Motskin M, Wright DM, Muller K, Kyle N, Gard TG, Porter AE, Skepper JN. Hydroxyapatite nano and microparticles: correlation of particle properties with cytotoxicity and biostability. Biomater. 2009;30:3307-3317.

[41] Wang L, Zhou G, Liu H, Niu X, Han J, Zheng L, Fan Y. Nano-hydroxyapatite particles induce apoptosis on MC3T3-E1 cells and tissue cells in SD rats. Nanoscale. 2012;4:2894-28999.

24

[42] Zhao X, Ng S, Heng BC, Guo J, Ma L, Tan TT, Ng KW, Loo SC. Cytotoxicity of hydroxyapatite nanoparticles is shape and cell dependent. Arch Toxicol. 2013;87:1037-1052.

[43] Liu D, Genetos D, Shao Y, Geist D, Li J, Ke HZ, Turner CH, Duncan RL. Activation of extracellular-signal regulated kinase (ERK1/2) by fluid shear is Ca2+- and ATP-dependent in MC3T3-E1 osteoblasts. Bone. 2008;42:644-652.

Figure captions
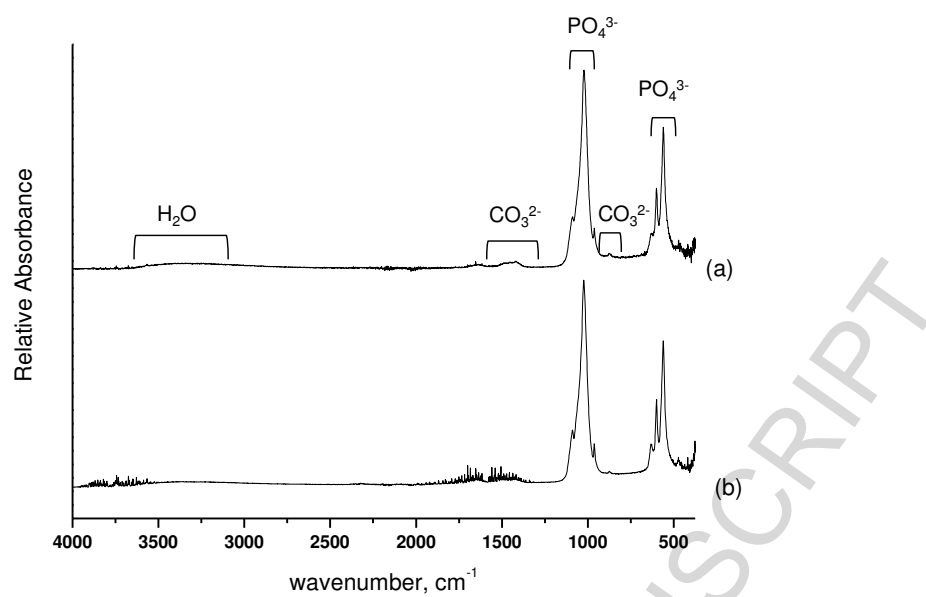
Fig. 1. Attenuated total reflectance Fourier transform infrared spectra of (a) BP-1 and (b) BP-2

materials.
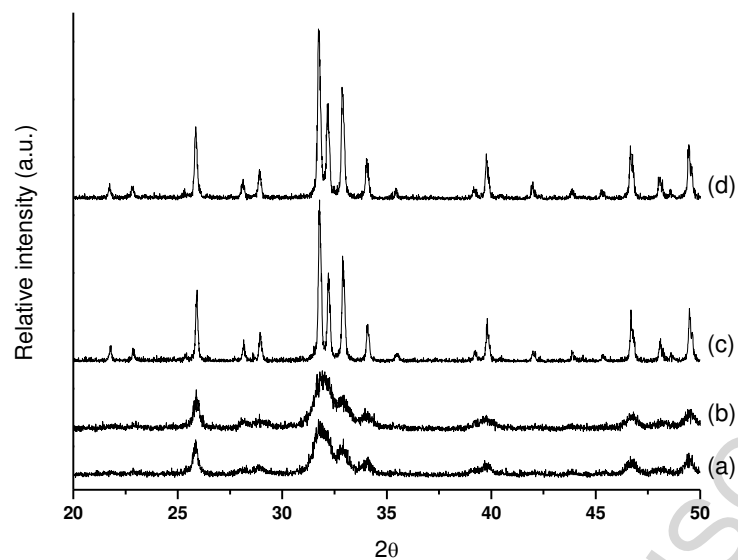
Fig. 2. X-ray powder diffraction patterns of BP-1 and BP-2 materials, (a) BP-1 paste, (b) BP-2 paste, (c) calcined BP-1 powder, (d) calcined BP-2 powder.
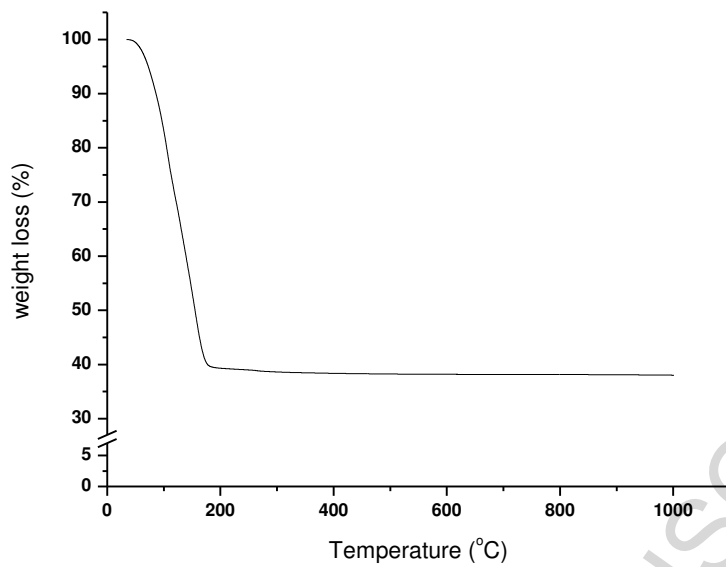
Fig. 3 Thermogravimetric analysis curve of BP-1 paste.
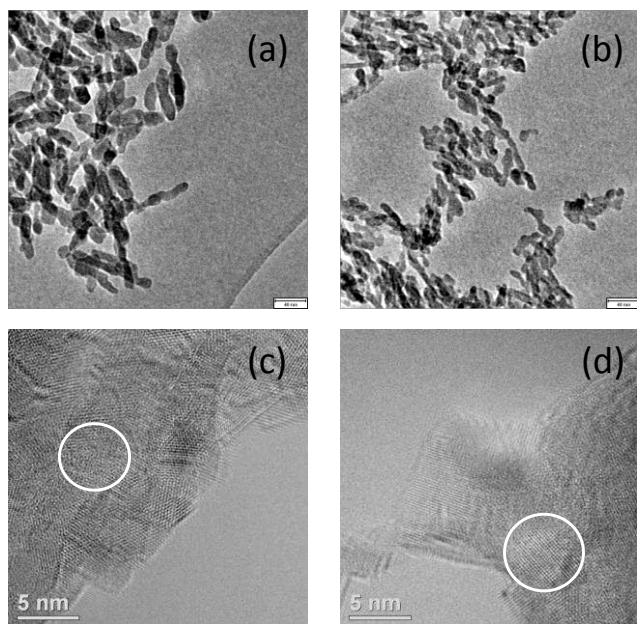
Fig. 4 Bright field transmission electron microscopy micrographs of (a) BP-1 and (b) BP-2 materials, scale bar 40 nm; HRTEM micrographs showing crystalline and amorphous regions in both (c) BP-1 and (d) BP-2, scale bar 5 nm.
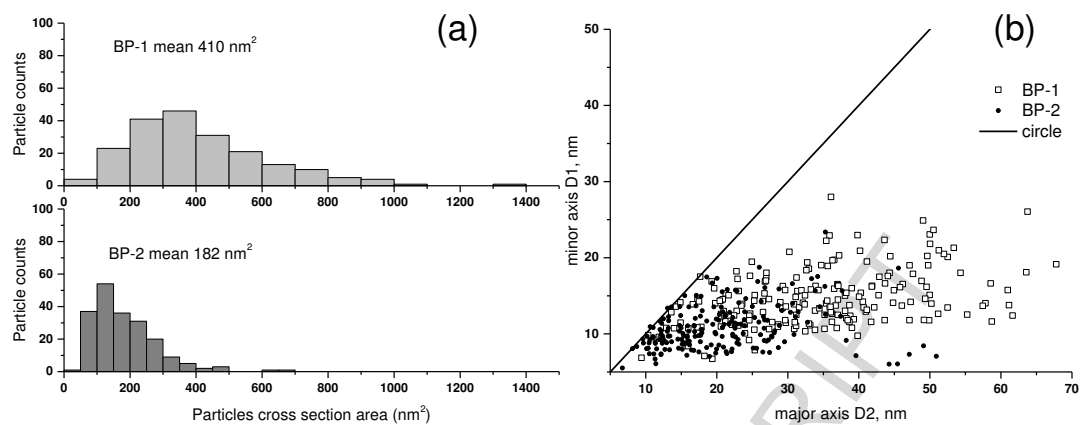
Fig. 5 Particle size analysis for BP-1 and BP-2 materials: (a) Projected area histograms and (b) aspect ratio evaluations.
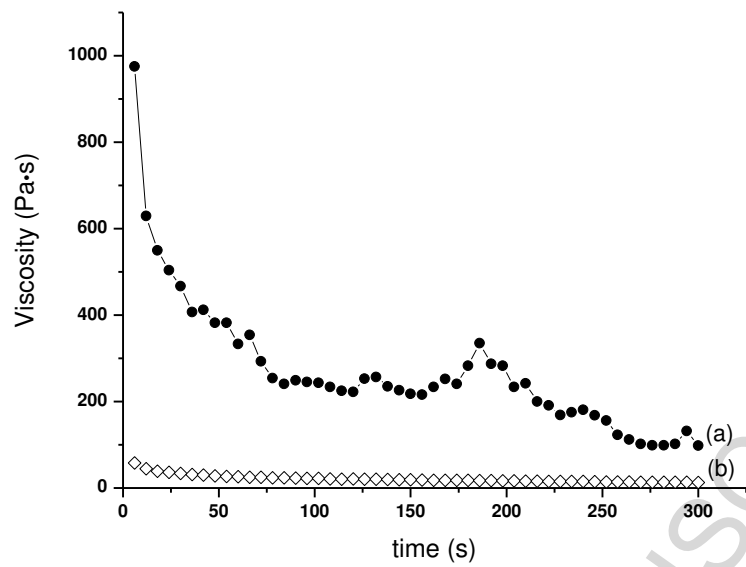
Fig. 6 Rheological test of (a) BP-2 and (b) BP-1 at constant shear rate of 10 s^{-1} and temperature 20 °C.

Table 1. Temperature dependence of the initial viscosity of BP-1 paste.

| Temperature	0 °C	10 °C	20 °C	25 °C	30 °C	37 °C	60 °C
Viscosity, Pa·s	66300 ±9%	68633 ±6%	84233 ±7%	93967 ±6%	89800 ±8%	109333 ±6%	112000
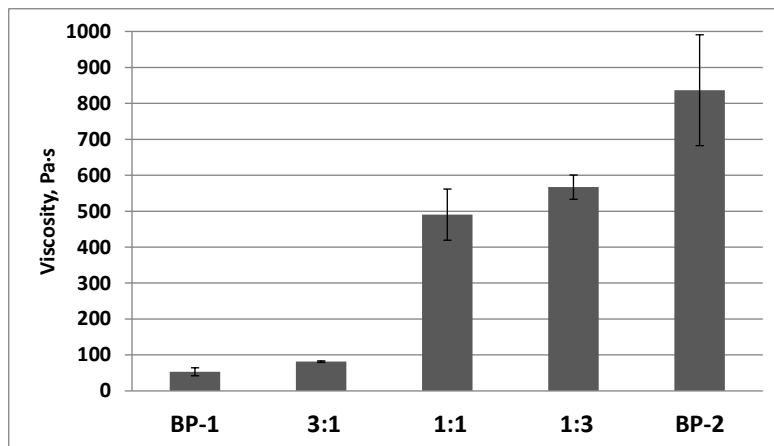
Fig. 7 Initial viscosity at different ratios of BP-1 and BP-2
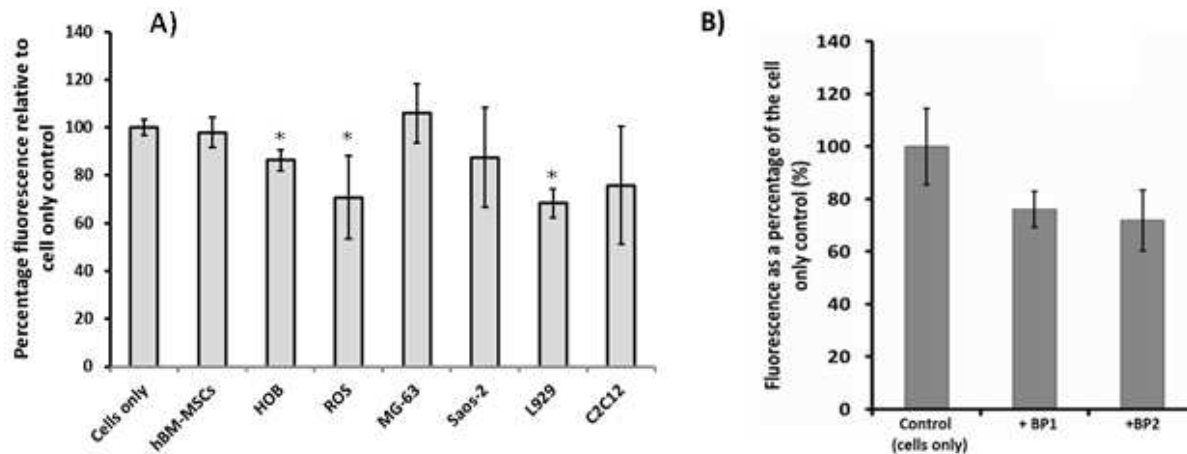
Fig. 8 Effect of BP-1 on the viability of osteoblastic and fibroblastic cells after 24 h incubation with paste conditioned media; (a) Effect on human primary cells (BM-MSCs, HOBs), and human osteoblastic cell-lines (MG 63, Saos-2), rat osteoblastic cell line (ROS), mouse fibroblast cell line (L929) and the mouse myoblast cell line, C2C12). (b) Comparison of the effect of BP-1 and BP-2 on the viability of MG63 osteoblastic cells.